Nonlinear optical endoscopy based on a double-clad photonic crystal fiber and a MEMS mirror

Ling Fu[a], Ankur Jain[b], Huikai Xie[b], Charles Cranfield[a], and Min Gu[a]

[a]*Centre for Micro-Photonics, Faculty of Engineering and Industrial Sciences,
Swinburne University of Technology, P. O. Box 218, Hawthorn, Victoria 3122, Australia*
[b]*Department of Electrical and Computer Engineering, University of Florida, Gainesville, FL 32611, USA*
mgu@swin.edu.au

Abstract: Two-photon fluorescence and second harmonic generation microscopy have enabled functional and morphological *in vivo* imaging. However, *in vivo* applications of those techniques to living animals are limited by bulk optics on a bench top. Fortunately, growing functionality of fiber-optic devices and miniaturization of scanning mirrors stimulate the race to develop nonlinear optical endoscopy. In this paper, we report on a prototype of a nonlinear optical endoscope based on a double-clad photonic crystal fiber to improve the detection efficiency and a MEMS mirror to steer the light at the fiber tip. The miniaturized fiber-optic nonlinear microscope is characterized by rat esophagus imaging. Line profiles from the rat tail tendon and esophagus prove the potential of the technology in *in vivo* applications.

© 2006 Optical Society of America

OCIS codes: (110.0180) Microscopy; (180.2520) Fluorescence microscopy; (110.2350) Fiber optics imaging

References and links

1. W. R. Zipfel, R. M. Williams and W. W. Webb, "Nonlinear magic: multiphoton microscopy in the biosciences," Nat. Biotechnol. **21**, 1369-1377 (2003).
2. P. J. Campagnola and L. M. Loew, "Second-harmonic imaging microscopy for visualizing biomolecular arrays in cells, tissues and organisms," Nat. Biotechnol. **21**, 1356-1360 (2003).
3. F. Helmchen, M. S. Fee, D. W. Tank and W. Denk, "A miniature head-mounted two-photon microscope: High-resolution brain imaging in freely moving animals," Neuron **31**, 903-912 (2001).
4. D. Bird and M. Gu, "Compact two-photon fluorescence microscope based on a single-mode fiber coupler," Opt. Lett. **27**, 1031-1033 (2002).
5. D. Bird and M. Gu, "Two-photon fluorescence endoscopy with a micro-optic scanning head," Opt. Lett. **28**, 1552-1554 (2003).
6. J. C. Jung, A. D. Mehta, E. Aksay, R. Stepnoski and M. J. Schnitzer, "In vivo mammalian brain imaging using one- and two-photon fluorescence microendoscopy," J. Neurophysiology **92**, 3121-3133 (2004).
7. M. J. Levene, D. A. Dombeck, K. A. Kasischke, R. P. Molloy, and W. W. Webb, "In vivo multiphoton microscopy of deep brain tissue," J. Neurophysiology **91**, 1908-1912 (2004).
8. L. Fu, X. Gan, and M. Gu, "Use of single-mode fiber coupler for second-harmonic-generation microscopy," Opt. Lett. **30**, 385-387 (2005).
9. D. Kim, K. H. Kim, S. Yazdanfar and P. T. C. So, "Optical biopsy in high-speed handheld miniaturized multifocal multiphoton microscopy," in *Multiphoton Microscopy in the Biomedical Sciences V*, A. Periasamy and P. T. C. So, eds., Proc. SPIE **5700**, 14-22 (2005).
10. B. A. Flusberg, J. C. Jung, E. D. Cocker, E. P. Anderson, and M. J. Schnitzer, "In vivo brain imaging using a portable 3.9 gram two-photon fluorescence microendoscope," Opt. Lett. **30**, 2272-2274 (2005).
11. J. Y. Ye, M. T. Myaing , T. P. Thomas, I. Majoros, A. Koltyar, J. R. Baker, W. J. Wadsworth, G. Bouwmans, J. C. Knight, P. St. J. Russell, and T. B. Norris, "Development of a double-clad photonic crystal fiber based scanning microscope," in *Multiphoton Microscopy in the Biomedical Sciences V* , A. Periasamy and P. T. C. So, eds., Proc. SPIE **5700**, 23-27 (2005).
12. L. Fu, X. Gan, and M. Gu, "Nonlinear optical microscopy based on double-clad photonic crystal fibers," Opt. Express **13**, 5528-5534 (2005). http://www.opticsexpress.org/abstract.cfm?URI=OPEX-13-14-5528.
13. H. Xie, Y. Pan, and G. K. Fedder, "Endoscopic optical coherence tomographic imaging with a CMOS-MEMS micromirror," Sens. Actuators **103**, 237-241 (2003).

14. H. Xie, A. Jain, T. Xie, Y. Pan, and G. K. Fedder, "A single-crystal silicon-based micromirror with large scanning angle for biomedical applications," Conference on Lasers and Electro Optics 2003, Baltimore, MD (2003).
15. P. Tran, D. Mukai, M. Brenner, and Z. Chen, "In vivo endoscopic optical coherence tomography by use of a rotational microelectromechanical system probe," Opt. Lett. **29**, 1236-1238 (2004).
16. P. Herz, Y. Chen, A. Aguirre, K. Schneider, P. Hsiung, J. Fujimoto, K. Madden, J. Schmitt, J. Goodnow, and C. Petersen, "Micromotor endoscope catheter for in vivo, ultrahigh-resolution optical coherence tomography," Opt. Lett. **29**, 2261-2263 (2004).
17. A. D. Aguirre, P. R. Herz, Y. Chen, J. G. Fujimoto, W. Piyawattanametha, L. Fan, S. Hsu, M. Fujino, M. C. Wu, and D. Kopf, "Ultrahigh resolution OCT imaging with a two-dimensional MEMS scanning endoscope," in *Advanced Biomedical and Clinical Diagnostic Systems III*, T. Vo-Dinh, W. S. Grundfest , D. A. Benaron, and G. E. Cohn, eds., Proc. SPIE **5692**, 277-282 (2005).
18. M. George, "Optical methods and sensors for in situ histology in surgery and endoscopy," Min. Invas. Ther. & Allied. Technol. **13**, 95-104 (2004).
19. L. Fu, X. Gan, and M. Gu, "Characterization of the GRIN lens-fiber spacing toward applications in two-photon fluorescence endoscopy," Appl. Opt. **44**, 7270-7274 (2005).
20. A. Jain, A. Kopa, Y. Pan, G. K. Fedder and H. Xie, "A two-axis electrothermal micromirror for endoscopic optical coherence tomography," *IEEE journal of selected topics in Quantum electronics* **10**, 636-642 (2004).

1. Introduction

Since its inception, multi-photon microscopy has emerged as one of the best non-invasive means of fluorescence microscopy [1]. Compared with its single-photon counterpart, two-photon fluorescence excitation offers an inherent optical sectioning property, a great penetration depth, and a flexible spectra accessibility for most fluorophores. Furthermore, accompanied nonlinear scattering processes such as second harmonic generation (SHG) from non-centrosymmetric structures, enable complementary information to visualize endogenous structures in tissues [2].

To further extend the *in vivo* applications of multi-photon microscopy, miniaturized microscopes have been developed to perform two-photon excited fluorescence (TPEF) and SHG imaging [3-12]. However, there are major obstacles which make them difficult to be applicable within internal cavities of the body. First, the scanning mechanisms are bulky and slow. Second, rigid probes based on combined gradient-index (GRIN) rod lenses can be inserted into deep tissues, but are not flexible to be incorporated into endoscopes to image internal organs. Finally, if a single-mode optical fiber or a fiber bundle is adopted to deliver a laser beam and collect signals, the low numerical aperture (NA) and the finite core size of the fibers give rise to a restricted sensitivity of the system. A possible way to overcome these obstacles is to guide excitation and emission beams using a length of fiber that exhibits two efficient transmission paths for excitation and emission wavelengths and to manipulate the optical beam by a micromirror with a diffraction-limited focus spot.

Recent advances in photonic crystal fibers (PCFs) [11, 12] and microelectromechanical system (MEMS) technology [13-17] offer a great possibility to achieve such a nonlinear optical endoscope that allows high-resolution imaging of internal organ systems. The previous study [12] demonstrates the detection efficiency of the double-clad PCF-based microscope is approximately 40 times higher than that in the single-mode-fiber-based microscope, mainly due to the large core size and high NA of the inner cladding. In this paper, we report a miniaturized nonlinear optical microscope based on a double-clad PCF and a MEMS scanning mirror. This MEMS-based single-fiber endoscopic nonlinear optical imaging probe is small with built-in MEMS scanning. The endoscope-based line profiles from rat tail tendon and esophagus have been successfully obtained, which demonstrates the promising potential for developing a real-time nonlinear optical endoscope to enable early cancer detection at the cellular level.

2. Endoscope design

An ultra-small probe head is designed to fit the working channel of a flexible endoscope and connect to the bulk optical components via a flexible fiber, as shown in Fig. 1(a). The double-clad PCF (Crystal Fiber A/S) has a core diameter of 20 µm, an inner cladding with a diameter of 165 µm and NA of 0.6 at wavelength 800 nm. This PCF plays a dual role to offer the robust single-mode guidance of near-infrared light in the central core and the efficient propagation of visible light within the multimode inner cladding. The central core is formed by air holes with a hole to hole pitch ratio of 0.26. A ring of air holes is used to efficiently guide and collect light in the pure silica multimode inner cladding. A laser beam generated from a Ti:Sapphire laser (Spectra Physics, Mai Tai) with a repetition rate of 80 MHz and a pulsewidth of approximately 80 fs is coupled through an iris diaphragm and a microscope objective CO (0.65 NA, 40X) into the fiber. Figure 1(b) is the output pattern from the fiber at wavelength 800 nm overlaid on the scanning electron microscopy (SEM) image of the double-clad PCF, indicating the single-mode operation in the central core and mode propagation within the inner cladding [12].
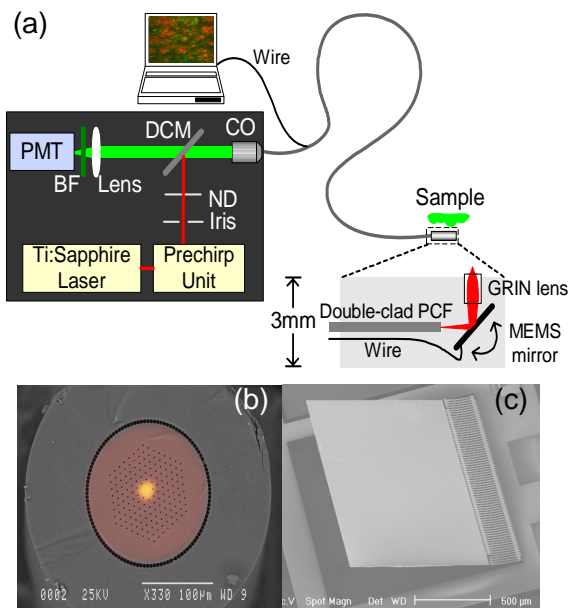

Fig. 1. (a) Schematic diagram of the nonlinear optical endoscope. The endoscope probe is based on a double-clad PCF, a MEMS mirror, and a GRIN lens. (b) A far-field output pattern from a double-clad PCF at wavelength 800 nm overlaid on a SEM image. (c) A SEM image of the MEMS

The excitation laser beam coupled from the double-clad PCF is reflected and scanned one-dimensionally by a MEMS mirror [Fig. 1(c)] with a maximum rotation angle of 17 degrees [14]. The MEMS mirror is based on electrothermal bimorph actuation and thus can achieve large rotation angles at low driving voltages. The mirror plate is 1 mm by 1mm in size, coated with aluminium for broadband high reflectivity. The mirror surface is flat due to a thick single-crystal silicon layer underneath. The radius of curvature of the mirror surface is about 0.5 m. It has a resonance frequency of 165 Hz, exceeding the scanning speed and angle requirements for most endoscopic applications [18]. The mirror scans at a frequency of 1 Hz in our experiment. A 0.2-pitch GRIN lens (GRINTECH) is used to focus the scanned laser beam at its back surface onto a sample, resulting in a working distance of approximately 150

μm. Unlike a conventional lens using curved surfaces to refract light, a GRIN lens uses a radial refractive index profile of nearly parabolic shape to guide light with a cosine ray trace. GRIN lenses are usually submillimeter in size and enormously flexible to meet various imaging requirements with low cost. As a consequence, the endoscope head of the prototype system is approximately 3 mm in diameter, equipped with the MEMS mirror and the GRIN lens.

3. Axial resolution and signal level

One of the advantages of nonlinear optical microscopy is its intrinsic optical sectioning ability in a thick sample. To estimate the axial resolution of the endoscope, we measure the axial responses of the system by scanning a thin layer of AF-50 dye in the z direction. It should be pointed out that the axial resolution and the signal level of the system varies as a function of the gap length between the fiber and the back surface of the GRIN lens, as shown in Fig. 2(a). When the gap length is approximately 5 mm to fulfill the back surface of the 0.5 mm-diameter GRIN lens, the optimized axial resolution of TPEF and SHG at an excitation wavelength of 800 nm for the system is approximately 6 μm and 5.4 μm, respectively, depicted in the inset of Fig. 2(b). In this case, the lateral resolution for nonlinear optical imaging is approximately 1 μm. The dependence of the peak intensity of TPEF and SHG axial responses on the excitation power on a log-log scale is illustrated in Fig. 2(b), demonstrating the quadratic dependence of the nonlinear optical signals and the efficient propagation through the double-clad PCF.
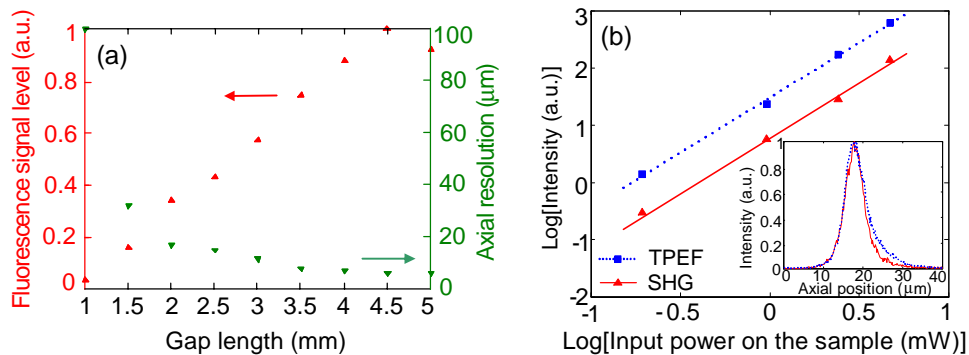
Fig. 2. (a) Detected intensity and axial resolution of two-photon fluorescence as a function of gap length. (b). Quadratic dependence of TPEF and SHG intensity on the excitation power. The inset show the axial responses of TPEF and SHG at 800 nm. A GRIN lens used for imaging has a diameter of 0.5 mm and a NA of 0.5.

It is found that the optimized signal level of the endoscope is approximately 160 times higher than that of the single-mode-fiber-based two-photon fluorescence endoscope [19]. The enhancement of the signal level results from the high NA and the large core diameter in the inner cladding of the double-clad PCF. In particular, the double-clad PCF offers more efficient signal collection as a function of the gap length, compared with the "trade-off" feature in the microscope using a single-mode fiber coupler and a GRIN lens [19]. In the configuration with a single-mode fiber coupler, optimization of axial resolution and optimization of signal level have to be achieved at separate gap lengths [19]. However, simultaneous optimizations of axial resolution and signal level can be obtained by use of double-clad PCFs. Additionally, the use of a prechirp unit consisting of a pair of gratings [Fig. 1(a)] can further increase the signal level by one order of magnitude.

4. Tissue imaging using a GRIN lens

To prove the effectiveness of a single GRIN lens for endoscopy, the *in vitro* nonlinear optical images from a rat esophagus tissue have been achieved using a double-clad PCF, a GRIN lens, and a 2-D scanning stage. Fig. 3 is the z projection of a series of sections from rat esophagus at an excitation wavelength of 800 nm, where Acridine Orange (1%, Sigma) is used to label nucleic acids to give TPEF contrast. Only SHG signals from connective tissue can be observed to exhibit the morphology of the micro-structures. In the rat esophagus tissue, the *in vitro* SHG signal originating from collagen is detectable using the double-clad
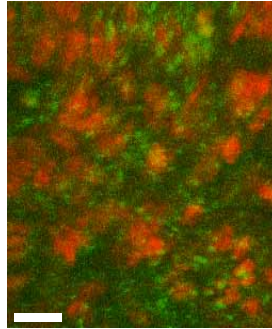

Fig. 3. Z projection of 8 slices through the rat esophagus tissue stained with Acridine Orange. 3-D movie for rat eshophagus tissue imaging is shown as m1 in supporting online material. Two-photon fluorescence (red) and SHG (green) visualize cell nuclei and connective tissue, respectively. A GRIN lens used for imaging has a diameter of 0.5 mm and a NA of 0.5. The excitation power on the sample resulting in two-photon fluorescence and SHG signals is 10 mW and 25 mW, respectively. Slice spacing is 5 µm. Scale bar represents 20 µm.

PCF and the 0.2-pitch GRIN lens, demonstrating the potential of SHG in diagnosis of collagen-related diseases.

5. Endoscopic imaging using a MEMS mirror

Rat tail tendon is used to characterize the nonlinear optical endoscope which is comprised of the double-clad PCF, the GRIN lens, and the MEMS mirror. Rat tail tendon consists of abundance of Type I collagen fibrils, which can be modelled in wound healing, malignancy, and development. Fig. 4(a) illustrates a series of SHG line profiles from rat tail tendon with a depth spacing of 10 µm. In this case, a 0.2-pitch GRIN lens having a diameter of 1 mm is used and the field of view on the sample is approximately 35 µm which corresponds to an optical scanning angle of approximately 6 degrees of the MEMS mirror. Only 5 V is needed to obtain 6-degree rotation. In our experiments, as the laser beam is scanned at the back surface of the GRIN lens, the GRIN lens is underfilled and results in an axial resolution of approximately 10 µm. The performance of the system (optical sectioning ability and line intensity) is consistent with that in a system using a bulk scanning stage [12]. Further, a SHG line profile from the rat esophagus tissue is shown in Fig. 4(b). The rat esophagus was removed from a euthanized rat, immersed in Hank's balanced salt solution (no phenol red) and imaged directly without any staining. The excitation power on the sample resulting in SHG signals is approximately 30 mW. Fig. 4(b) confirms that the nonlinear optical endoscope probe based on the double-clad PCF, the GRIN lens and a MEMS mirror enables rat esophagus imaging *in vitro*.
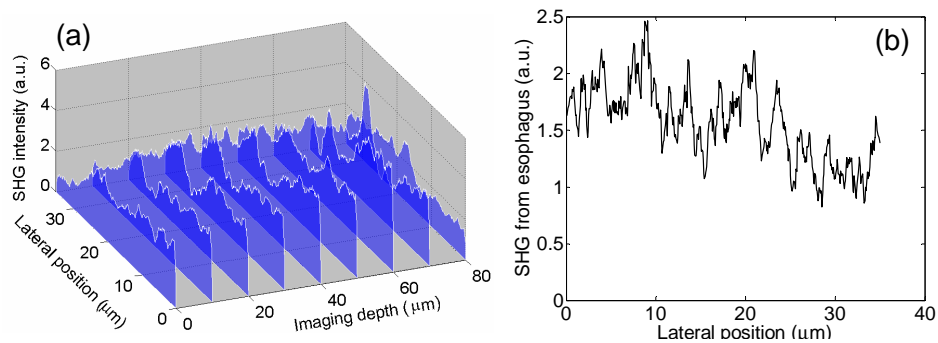
Fig. 4. (a) A series of SHG line profiles taken at a 10-μm step into rat tail tendon. (b) A SHG line profile from unstained rat esophagus tissue.

6. Conclusion

We have demonstrated experimentally the concept of nonlinear optical endoscopy based on a double-clad PCF, a GRIN lens and a MEMS mirror. A double-clad PCF has been used to deliver the pulsed excitation beam and collect nonlinear optical signals with a detection efficiency enhanced by 160 times. Using a MEMS mirror as the scanning unit and a GRIN lens to produce a fast scanning focal spot offers a great potential to develop a compact endoscope probe for *in vivo* applications. To our best knowledge, our result is the first report on nonlinear optical imaging of unstained rat esophagus tissue with a miniaturized nonlinear optical microscope based on a single fiber and a MEMS mirror. The technology will enable visualizations of functional and morphological changes of tissue at the microscopic level rather than direct observations with a traditional instrument at the macroscopic level. It could be a complement for conventional multi-photon microscopy and optical coherent tomography [15-17]. Further integration of a 2-D MEMS mirror [20] and a large diameter GRIN lens will allow for real-time imaging with a field of view up to a hundred micrometers. We therefore expect the nonlinear optical endoscope to complement other endoscopic imaging and enable optical biopsy for early cancer detection.

Acknowledgments